Journal of Experimental and Applied Physics
Journal Homepage: jeap.ppj.unp.ac.id
Vol. 2, No. 1, March 2024.
ISSN (Print): 2988-0378 ISSN (Online): 2987-9256

Earthquake Intensity Determination Based on Maximum Land Acceleration in Padang City Area Using Atkinson Boore Method (2003)

Linda Susanti[1], Syafriani[1*], Hamdi[1], Letmi Dwiridal[1]

Department of Physics, Universitas Negeri Padang, Padang 25131, Indonesia

Article History
Received : February, 9th 2024
Revised : March, 2nd 2024
Accepted : March, 31st 2024
Published : March 31st, 2024

DOI:
https://doi.org/10.24036/jeap.v2i1.40

Corresponding Author
*Author Name: Syafriani
Email: syafri@fmipa.unp.ac.id

Abstract: Geologically, the City of Padang had the potential for large earthquake impacts due to its location within the Sumatran Fault, Mentawai Fault, and above the Subduction Zone. The magnitude of earthquake damage was determined by soil quality factors and earthquake intensity. To determine the extent of damage, the maximum ground acceleration value was used. This value represented the maximum ground vibration acceleration that occurred at a specific location within a particular area, resulting from all earthquakes that occurred during a specific time period. The maximum ground acceleration value and earthquake intensity in the Padang City area could be calculated using the Atkinson Boore (2003) method. This study was a quantitative research that commenced by examining relevant theories related to the issue at hand. The research then proceeded with the collection of secondary data obtained from the United States Geological Survey (USGS) website. Specifically, earthquake data for the period between 2000 - 2020 in the Padang City area with coordinates $\mathbf{0^o44'}$ LS- $\mathbf{1^o08'}$ LS and $\mathbf{100^o05'}$ BT- $\mathbf{100^o34'}$ BT, and a magnitude M ≥ 5.0 SR depth < 100 km were utilized. Historical earthquake data was employed to determine earthquake intensity values, which were then used to assess the earthquake risk in the Padang City area. Based on the calculation results, the maximum acceleration value of soil was found between 0.519001g - 0.603847g. The highest value of maximum acceleration of soil was located in Bungus Teluk Kabung area, while the lowest value was found in Koto Tangah area. The distribution of earthquake intensity (MMI) in Kota Padang area has a value of VIII MMI.

Keywords: Atkinson Boore; Earthquake Intensity; Maximum Ground.

How to cite:
L. Susanti, Syafriani, Hamdi, and L. Dwiridal, 2024, Earthquake Intensity Determination Based on Maximum Land Acceleration in Padang City Area Using Atkinson Boore Method (2003), *Journal of Experimental and Applied Physics,* Vol.2, No.1*,* page 48-59.

1. Introduction

Indonesia is an areas where three tectonic plates meet (Triple Junction Plates), name the Indo-Australian plate, in the Eurasian plate and the Pacific plate. The Indo-Australian plate collides with the Eurasian plate off the coast of Sumatra, Java and Nusa Tenggara, while with the Pacific in North Irian and North Maluku [1]. Indonesia is a country that is no stranger to earthquake disasters. BNPB recorded 8,624 times in 2020, 11,515 earthquakes occurred in 2019, 11,920 times in 2018. Several supporting factors, namely geological factors including soil and rock types, soil structure and texture, topography, tectonics, and river flow patterns [2]. An earthquake is defined as a sudden and very rapid shaking of the ground due to the sudden release of energy in the earth's crust [3]. Earthquakes are events of ground shaking caused by the sudden release of seismic waves from a source of elastic energy and the rock located at the source of the earthquake cannot withstand the force caused by the relative movement of the rock plates where the force is located and the resistance between them. Rocks are used to determine the magnitude of an earthquake that will occur [4].

The energy obtained from an earthquake event can be created from all kinds of different sources, such as volcanic eruptions, movement of the earth's plates and human activities or the collapse of a cave underground. The occurrence of tectonic earthquakes can be described by the theory of the movement of tectonic plates on a large scale. The theory of plate tectonics illustrates that the presence of an earthquake is a sign or symptom of an active tectonic shift, this can be seen by most of the seismic activity that occurs at plate boundaries [5]. The hypocenter is the location at depth where the earthquake first occurred. The epicenter is the point on the surface directly above the hypocenter of an earthquake, the epicenter of an earthquake is called the hypocenter, which is located inside the earth [6]. Meanwhile, the center of the earth's vibrations is called the epicenter, which is located on the surface of the earth or on the seabed. Earthquakes can be categorized into the strength of the wave or vibration of the earthquake, the depth of the hypocenter and the source of the cause [7].

The area on the island of Sumatra is an earthquake-prone area due to its location adjacent to the subduction zone in the Indian Ocean. West Sumatra is tectonically an area prone to earthquakes because it is located at the confluence of the Indo-Australian plate subducting under the Eurasian Plate which forms the earthquake. The earthquake area in West Sumatra is in the subduction area, the Mentawai Fault and the Sumatran Fault [8,9]. The Padang City area is a city that has the potential for earthquakes because of its western coastal location facing the megathrust earthquake source zone, according to experts, it has quite a large magnitude potential. Soil and building quality factors are very determining factors for earthquake risk assessment. The quality of the soil where the building stands is expressed by the maximum ground acceleration (Peak Ground Acceleration) from the exact accelerograph record when a major earthquake occurs.

Peak Ground Acceleration (PGA*)* due to earthquakes is the maximum ground vibration acceleration that occurs at a point in a certain position in an area which is calculated as a result of all earthquakes that occur over a certain period of time taking into account the magnitude and distance of the hypocenter, and the dominant period of the ground where the point is [10]. Atkinson Boore (2003) attenuation method can be used for subduction earthquake sources in the megathrust and beniof zones. This attenuation relationship has also been developed by compiling a database of response spectra from strong ground vibration records with M=5 SR to M=8.5 SR that occur in subduction zones around the world, including interface and intraslab events.

The methods of Mc.Guirre R.K (2003), and Mickey (2003) have similarities, namely the equation uses earthquake parameters, namely, the earthquake epicenter point (latitude and longitude), magnitude and depth of the hypocenter. There are limitations to calculating ground acceleration values using this formulation, namely, the earthquake data used as a source is earthquake data that has a hypocenter depth of 9 - 70 km, with a magnitude of 5 SR which must later be converted into surface magnitude (Ms). Based on this explanation, research was carried out on ground acceleration in the Padang City area, West Sumatra using the Atkinson Boore method, because this method is able to provide an overview of ground acceleration values in general and this method is in accordance with the data the author uses, namely based on historical earthquake data[10].

Another factor that can influence the ground acceleration value is the level of soil density in the area. So, the resulting ground acceleration is directly proportional to the magnitude and inversely proportional to the epicenter, distance, soil density, and depth of the hypocenter. Maximum ground acceleration is defined as a measure of the spread of ground acceleration in an area caused by earthquake vibrations within a certain time [11]. This ground acceleration value can be useful in showing the impact of physical damage that needs to be estimated in planning efforts to make buildings that are earthquake resistant [12]. Buildings that are strong against earthquakes will minimize building damage and loss of life. Damage to buildings caused by earthquakes is influenced by building parameters and ground movement parameters. Building parameters can be seen in the characteristics of materials and building structural elements, while the parameters of ground movement depend on the magnitude, distance, mechanism, and local soil conditions [13]. Classification of disaster risk levels can be done by scoring, namely by making mathematical calculations by multiplying the weights and class scores that have been planned.

2. Materials and Method

Based on the background and research objectives to determine the risk of earthquakes based on the maximum ground acceleration value in the Padang City area using the Atkhinson Boore (2003) method with a quantitative descriptive research type. The descriptive method is a method of examining the status of human groups, an object, a set of conditions, a system of thought, or a class of events in the present [14]. Quantitative research is research that refers to the philosophy of post positivism, applied to certain populations or samples to conduct research, data collection uses research instruments, and data analysis is quantitative, with the aim of testing the hypotheses that have been set. Flowchart for the atkinson boore method (2003) can be seen in Figure 1.

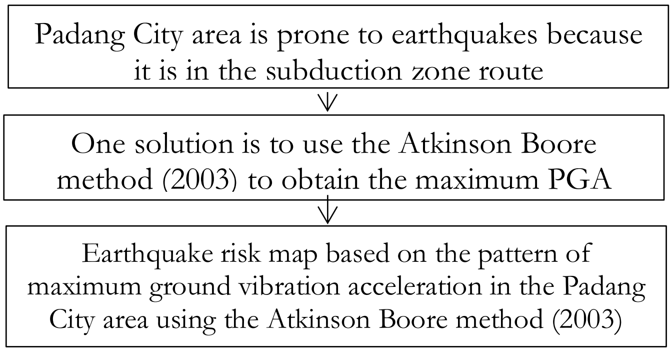

Figure 1. framework of thinking for the atkinson boore method (2003)

Based on Figure 1, the research data used is secondary data in the form of earthquake data obtained from the earthquake history of the Padang City area. Earthquake parameters used for the process of mapping the distribution of epicenters, hypocenter locations, mapping of maximum ground vibration acceleration maps, magnitude of earthquake intensity values, and mapping of earthquake risk maps that occur in the Padang City area. Data processing can first be done by making a grid in the Padang City area to determine research points, followed by finding the distance of the epicenter from each research point to the earthquake point using latitude and longitude data from each research point using equation 1.

$$D\mathit{fault} = (x_2 - x_1) + (y_2 - y_1) \tag{1}$$

Where Δ is the epicenter distance (degrees), y_2 is the calculation area latitude (degrees), y_1 is the earthquake epicenter latitude (degrees), x_2 is the longitude calculation area (degrees), x_1 and is the longitude of the earthquake epicenter (degrees). The epicenter distance obtained is made in kilometers with the conversion 1° is the 111 km. The hypocenter distance can be calculated by equation 2.

$$R=\sqrt{D^2 + H^2} \tag{2}$$

Where Δ is the epicenter distance (degrees), y_2 is the calculation area latitude (degrees), y_1 is the earthquake epicenter latitude (degrees), x_2 is the longitude calculation area (degrees), x_1 and is the longitude of the earthquake epicenter (degrees). The epicenter distance obtained is made in kilometers with the conversion 1° is the 111 km. The hypocenter distance can be calculated by equation 2.

$$\ln Y = C_1 + C_2(M-6) + C_3(M-6)^2 - lnR - c_4R + ln\varepsilon \tag{3}$$

Where Y is the ground vibration acceleration (PGA), M is the moment magnitude with M is the 8.5 (interface) with M >8.5 and M is the 8 (intraslab) with M >8.0, h is the depth of the earthquake source, if h >100 then h is the 100 km, c_1 is the 2,991, c_2 is the 0,03525, c_3 is the 0,00759, and c_4 is the -0,00206. Making a grid for the Padang City area was then continued by finding the distance of the epicenter from each grid to the earthquake point using latitude and longitude data from each grid. Calculating the hypocenter distance for each grid. After the hypocenter distance value has been obtained, we can calculate the maximum ground vibration acceleration value using the Atkinson Boore (2003) method using the magnitude value of the earthquake source. Finally, look for the maximum value in each earthquake event grid from the calculation results of the maximum ground vibration acceleration value.

3. Results and Discussion

The earthquake catalog data used in this study is sourced from the U.S. Geology Survey (USGS), namely earthquake data in the Padang City area in the 2000-2020 periods, sourced from the Mentawai Segment and its surroundings totaling 63 incidents. After the earthquake data is obtained, the next step is to select/filter the earthquake data according to the parameters of the Atkinson Boore method (2003). The parameters were the strength of the earthquake taken must be ≤ 5 on the Richter scale, the depth of the earthquake used is shallow earthquake depth, if the depth of the earthquake is <100 km, the earthquake is included in the category of subduction earthquake. The subduction zone or it can also be called subduction occurs due to subduction where the oceanic plate will dive under the continental plate. This is because oceanic crust is denser than volcanic crust.

Based on the data obtained, it shows that earthquakes in the Padang City area had a magnitude of 5-6.7 on the Richter scale and a depth of 10-48.42 km in 63 earthquake events in the period 2000 - 2020. This shows that the Padang City area is prone to earthquakes. The Padang City area is divided by 0°03'30" x 0°03'30" to obtain a grid map of the Padang City area. Where this data will be used to find the distance between the hypocenter and epicenter of the earthquake. A grid map of the Padang City area can be seen in Figure 2.

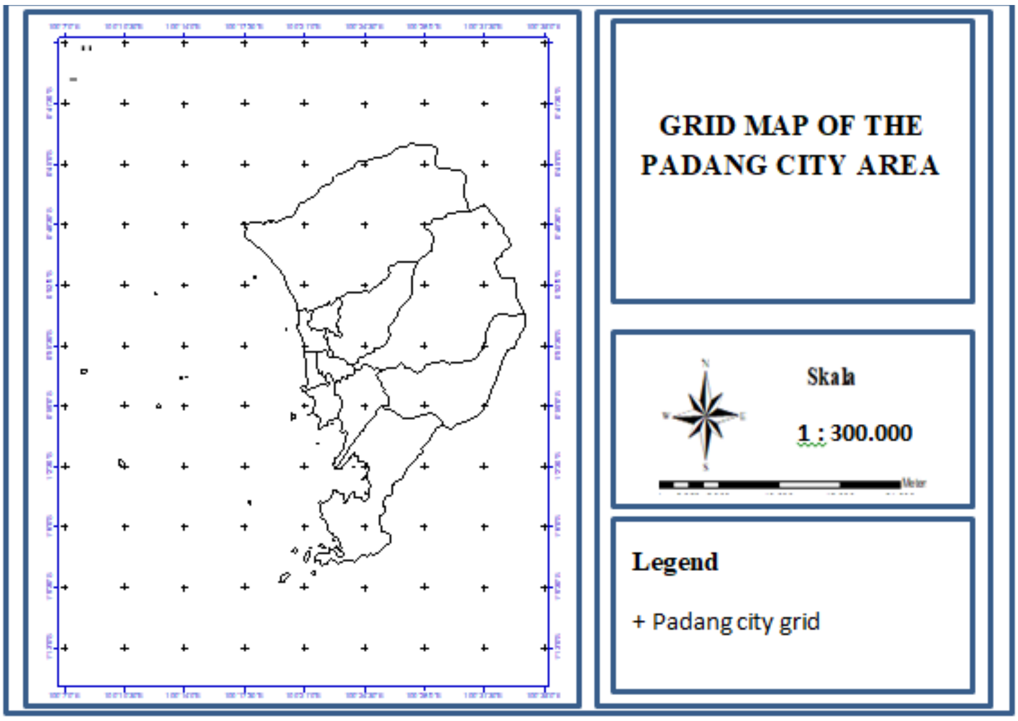

Figure 2. Grid map of the Padang City area

Based on Figure 2, there were 99 calculation grids obtained from the results of dividing the Padang City area with a distance of 0°03'30" x 0°03'30". Each point is calculated for the maximum ground acceleration value from earthquake data originating from the Mentawai segment and its surroundings in 2000-2020 with a magnitude of > 5 SR and a depth of < 100 km with coordinate boundaries of 0°44' LS - 1°08' LS and 100°05' BT - 100°34' BT. The research point will be used to determine the distance from the epicenter and hypocenter of the earthquake in the Padang City area. The distribution of earthquakes can be seen in Figure 3.

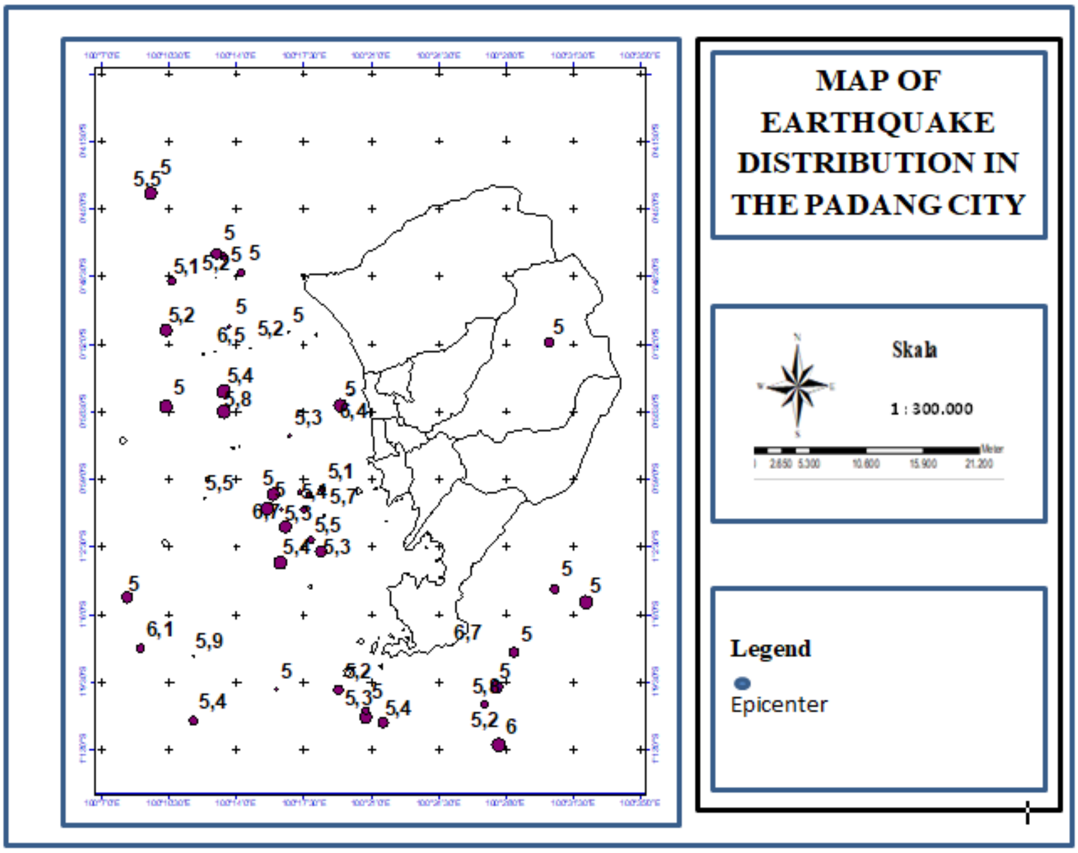

Figure 3. Map of the distribution of earthquakes in the offshore sea area around the City of Padang

Figure 3 shows the distribution of earthquakes in the period 2000 to 2020 obtained in the U.S. Geological Survey (USGS). It can be seen in Figure 3 that earthquakes were widely spread in the western and southern parts of Padang City area with magnitudes ranging from 5 SR-6.7 SR from 63 earthquake events. This data will be used to determine the maximum ground acceleration value in the Padang City area using the Atkhinson Boore (2003) method which can be seen in equation 3 [15]. Equation 1 where for c1 is the 2.991, c2 is the 0.03525, c3 is the 0.00759, and c4 is the -0.00206, so that the maximum ground acceleration value is obtained in the Padang City area. The maximum ground acceleration value obtained can be seen in table 1.

Table 1. Maximum Ground Acceleration Value in the Padang City Area

Longitude	Latitude	PGA	Longitude	Latitude	PGA
100.1469	-1.13174	0.488268	100.1469	-0.91991	0.530203
100.1758	-1.13174	0.494487	100.1758	-0.91991	0.535331
100.2046	-1.13174	0.50053	100.2046	-0.91991	0.540341
100.2335	-1.13174	0.506406	100.2335	-0.91991	0.545239
100.2623	-1.13174	0.512125	100.2623	-0.91991	0.550029
100.2912	-1.13174	0.517695	100.2912	-0.91991	0.554717
100.32	-1.13174	0.523125	100.32	-0.91991	0.559308
100.3489	-1.13174	0.528421	100.3489	-0.91991	0.563805
100.3777	-1.13174	0.533591	100.3777	-0.91991	0.568213
100.4066	-1.13174	0.53864	100.4066	-0.91991	0.572536
100.4354	-1.13174	0.543576	100.4354	-0.91991	0.576777
100.4643	-1.13174	0.548402	100.4643	-0.91991	0.58094
100.4931	-1.13174	0.553125	100.4931	-0.91991	0.585027
100.522	-1.13174	0.557748	100.522	-0.91991	0.589041
100.5508	-1.13174	0.562277	100.5508	-0.91991	0.592986
100.1469	-1.08938	0.497339	100.1469	-0.87754	0.537692
100.1758	-1.08938	0.503303	100.1758	-0.87754	0.542649
100.2046	-1.08938	0.509104	100.2046	-0.87754	0.547495
100.2335	-1.08938	0.514752	100.2335	-0.87754	0.552237
100.2623	-1.08938	0.520255	100.2623	-0.87754	0.556879
100.2912	-1.08938	0.525622	100.2912	-0.87754	0.561426
100.32	-1.08938	0.530858	100.32	-0.87754	0.565881
100.3489	-1.08938	0.535971	100.3489	-0.87754	0.570249
100.3777	-1.08938	0.540966	100.3777	-0.87754	0.574533
100.4066	-1.08938	0.54585	100.4066	-0.87754	0.578736
100.4354	-1.08938	0.550627	100.4354	-0.87754	0.582863
100.4643	-1.08938	0.555302	100.4643	-0.87754	0.586916
100.4931	-1.08938	0.559881	100.4931	-0.87754	0.590898
100.522	-1.08938	0.564367	100.522	-0.87754	0.594811
100.5508	-1.08938	0.568764	100.5508	-0.87754	0.598658
100.1469	-1.04701	0.50604	100.1469	-0.83517	0.544932
100.1758	-1.04701	0.511768	100.1758	-0.83517	0.549729
100.2046	-1.04701	0.517347	100.2046	-0.83517	0.554424
100.2335	-1.04701	0.522786	100.2335	-0.83517	0.559021
100.2623	-1.04701	0.52809	100.2623	-0.83517	0.563524
100.2912	-1.04701	0.533268	100.2912	-0.83517	0.567937
100.32	-1.04701	0.538325	100.32	-0.83517	0.572266
100.3489	-1.04701	0.543267	100.3489	-0.83517	0.576512

Longitude	Latitude	PGA	Longitude	Latitude	PGA
100.3777	-1.04701	0.5481	100.3777	-0.83517	0.580679
100.4066	-1.04701	0.552829	100.4066	-0.83517	0.584771
100.4354	-1.04701	0.557459	100.4354	-0.83517	0.58879
100.4643	-1.04701	0.561993	100.4643	-0.83517	0.592739
100.4931	-1.04701	0.566437	100.4931	-0.83517	0.596621
100.522	-1.04701	0.570794	100.522	-0.83517	0.600439
100.5508	-1.04701	0.575068	100.5508	-0.83517	0.604194
100.1469	-1.00464	0.5144	100.1469	-0.79281	0.551941
100.1758	-1.00464	0.519912	100.1758	-0.79281	0.556589
100.2046	-1.00464	0.525287	100.2046	-0.79281	0.561141
100.2335	-1.00464	0.530531	100.2335	-0.79281	0.565602
100.2623	-1.00464	0.535651	100.2623	-0.79281	0.569975
100.2912	-1.00464	0.540654	100.2912	-0.79281	0.574264
100.32	-1.00464	0.545544	100.32	-0.79281	0.578473
100.3489	-1.00464	0.550328	100.3489	-0.79281	0.582605
100.3777	-1.00464	0.55501	100.3777	-0.79281	0.586662
100.4066	-1.00464	0.559595	100.4066	-0.79281	0.590648
100.4354	-1.00464	0.564086	100.4354	-0.79281	0.594566
100.4643	-1.00464	0.568489	100.4643	-0.79281	0.598417
100.4931	-1.00464	0.572806	100.4931	-0.79281	0.602205
100.522	-1.00464	0.577042	100.522	-0.79281	0.605932
100.5508	-1.00464	0.5812	100.5508	-0.79281	0.6096
100.1469	-0.96228	0.522446	100.1469	-0.75044	0.558733
100.1758	-0.96228	0.527759	100.1758	-0.75044	0.563242
100.2046	-0.96228	0.532944	100.2046	-0.75044	0.567661
100.2335	-0.96228	0.538009	100.2335	-0.75044	0.571995
100.2623	-0.96228	0.542958	100.2623	-0.75044	0.576246
100.2912	-0.96228	0.547798	100.2912	-0.75044	0.580418
100.32	-0.96228	0.552533	100.32	-0.75044	0.584514
100.3489	-0.96228	0.557169	100.3489	-0.75044	0.588538
100.3777	-0.96228	0.56171	100.3777	-0.75044	0.592492
100.4066	-0.96228	0.566159	100.4066	-0.75044	0.596378
100.4354	-0.96228	0.570522	100.4354	-0.75044	0.600199
100.4643	-0.96228	0.574801	100.4643	-0.75044	0.603958
100.4931	-0.96228	0.578999	100.4931	-0.75044	0.607657
100.522	-0.96228	0.583121	100.522	-0.75044	0.611298
100.5508	-0.96228	0.58717	100.5508	-0.75044	0.614882

Earthquake disasters can be minimized with early and optimal mitigation efforts, one of the mitigation efforts that needs to be done is to make a maximum ground acceleration map to determine the impact area of an earthquake which is useful in describing the effects of an earthquake at a location which will help in anticipation and minimizing casualties and material losses [16,17]. The results of the maximum ground acceleration map for Padang City area can be seen in Figure 4.

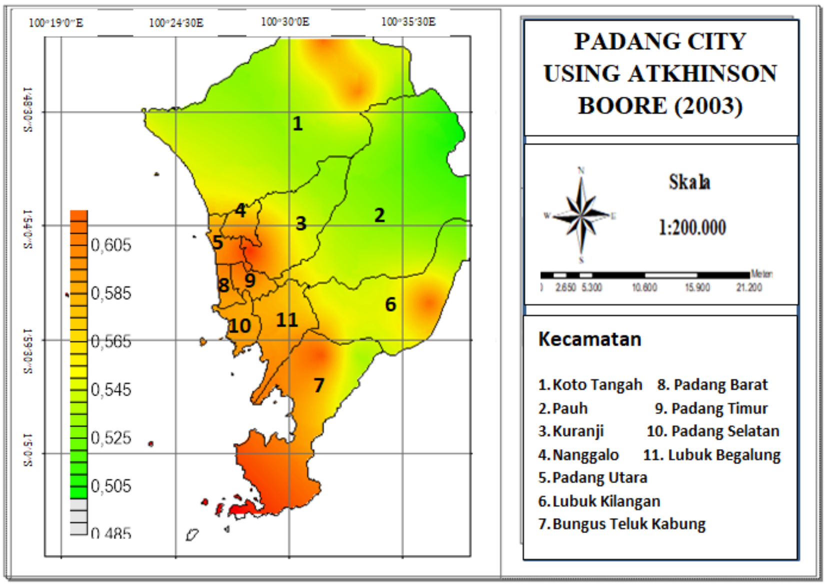

Figure 4. Map of maximum peak acceleration

Figure 4 shows the distribution of the maximum ground acceleration values for the Padang City area. Based on the maximum ground acceleration map, values with darker colors indicate a larger maximum ground acceleration value in the Padang City area. While the lighter color indicates smaller maximum ground acceleration, where the red color was the highest value and the green color was the lowest value. Damage caused by earthquakes must be predicted quickly with accurate tools, but there were several areas that did not meet these tools, so a maximum ground acceleration map was needed to determine areas prone to earthquakes [18].

The maximum ground acceleration value in the Padang City area will be linked to the earthquake intensity value to determine the area of damage caused by the earthquake in the Padang City area. The maximum intensity values obtained tend to be high in areas that have high maximum acceleration values as well. The geological structure factors in the area that have a relatively high maximum intensity were due to the regional geological conditions, namely alluvium deposits, metamorphic relief and low metamorphosed sedimentary rocks. Earthquake waves tend to be amplified in areas with young rock types or soft structures, whereas earthquake waves tend to be damped if they pass through hard rock structures and old rocks [19]. The grouping of earthquake intensity values based on the level of damage can be seen in table 2.

Table 2. Classification of Earthquake Intensity Values Based on the Level of Damage [20]

Intensitas	PGA	Perceived shaking	Potential damage
I	< 0,0017 g	Not felt	None
II – III	0,0017-0,014 g	Weak	None
IV	0,014-0,039 g	Light	None
V	0,039-0,092 g	Moderate	Very Light
VI	0,092-0,18 g	Strong	Light
VII	01,8-0,34 g	Very strong	Moderate
VIII	0,34-0,65 g	Severe	Moderate to heavy
IX	0,65-1,24 g	Violent	Heavy
X +	> 1,24 g	Extreame	Very heave

Based on table 2, the Padang City area can be grouped into was two areas, namely the vulnerable area and the alert area. The area with the highest maximum ground acceleration value was included in the vulnerable area group, while the area with the smallest ground acceleration value was included in the alert area group. The vulnerable area includes Bungus Teluk Kabung District, while the alert area includes parts of Koto Tangah District and Pauh District. The highest maximum ground acceleration values were in the Bungus Teluk Kabung, Lubuk Begalung, South Padang, West Padang, East Padang, North Padang, Nanggalo, Lubuk Kilangan and Kuranji areas, while the lowest maximum ground acceleration values were in the Pauh and Koto Tangah areas. The distribution of earthquake intensity values (MMI) for the Padang City area has a VIII MMI value.

Based on the calculation results show that Bungus Teluk Kabung District has the highest maximum ground acceleration value, while the lowest acceleration value was in Koto Tangah District. This was because Bungus Teluk Kabung District has a geological formation that was the dominated by alluvial deposits, where these deposits tend to crack more quickly and break apart so that if vibrations occur due to an earthquake, the area will experience quite severe damage. Whereas the Koto Tangah District has geological formations of Holocene-aged quaternary surface sedimentary rocks and tertiary volcanic rocks that was Pleistocene in age. So this will make the Padang City area grouped into two parts of the area, namely areas that were vulnerable and areas that will be on alert. The area with the highest maximum ground acceleration value was included in the group of areas prone to earthquakes, while the area with the lowest ground acceleration value will be included in the group of areas that were alert to earthquakes [21].

4. Conclusion

Based on the results of value calculation of the maximum ground acceleration value, several conclusions can be drawn: The maximum ground acceleration value in the Padang City area was between 0,519001g-0,603847g, this was because the Padang City area has the potential for earthquakes due to the Subduction Zone which was beneath the land. And the results of the maximum ground acceleration calculation and the maximum ground acceleration map in the Padang City area, the highest maximum ground acceleration values were in the Bungus Teluk Kabung area, Lubuk Begalung, South Padang, West Padang, East Padang, North Padang, Nanggalo, Lubuk Mills, and Kuranji. The distribution of earthquake intensity values (MMI) for the Padang City area has a VIII MMI value.

References

[1] H. Abbas, H. Nurbaeti, and A. Andi. "Earthquake disaster mitigation with the learning by doing method". Window of Health: Journal of Health, 5.1, 475–485. 2022. https://doi.org/10.33096/woh.vi.139
[2] R. J. Telford, and S. Kruse. 2022. "Reversals in temperature-precipitation correlations in the northern hemisphere extratropics during the holocene". Geophysical Research Lestters, 49.22, 1–11. https://doi.org/10.1029/2022GL099730
[3] Y. M. Kartikasari, and A. Choiruddin 2022. "Earthquake risk analysis in Sumatra with the cauchy cluster process". Inference, 5-2, 123. https://doi.org/10.12962/j27213862.v5i2.12307
[4] M. Flageat, F. Chalumeau, and A. Cully 2023. "Empirical analysis of PGA-MAP-Elites for neuroevolution in uncertain domains". ACM Transactions on Evolutionary Learning and Optimization, 3.1, 1–32. https://doi.org/10.1145/3577203
[5] M. A Bening, D. P. Sahara, W. Triyoso, and, D. Kusumawati 2022. "Modeling the impact of the viscoelastic layer thickness and the frictional strength to the lithosphere deformation in a strike-slip fault: insight to the seismicity pattern along the great Sumatran Fault". GeoHazards, 3.4, 452–464. https://doi.org/10.3390/geohazards3040023
[6] W. Zhu, McBrearty, I. W., Mousavi, S. M, W. L. Ellsworth, and, G. C. Beroza "Earthquake phase association using a bayesian gaussian mixture model". Journal of Geophysical Research: Solid Earth, 127.5, 1–16. 2022. https://doi.org/10.1029/2021JB023249
[7] M. N. Adlini, A. H. Dinda, S. Yulinda, O. Chotimah, and, S. J. Merliyana "Literature study qualitative research methods". Edumaspul: Journal of Education, 6.1, 974–980. 2022. https://doi.org/10.33487/edumaspul.v6i1.3394
[8] J. B. Ammirati, A. Villaseñor, S. Chevrot, G. Easton, M. Lehujeur, S. Ruiz, and M. C. Flores. "Automated earthquake detection and local travel time tomography in the south-central andes (32–35°S): implications for regional tectonics". Journal of Geophysical Research: Solid Earth, 127.4. 2022. https://doi.org/10.1029/2022JB024097
[9] M. M. Hason, A. H. Zuhairi, A. N. Hanoon, A. A. Abdulhameed, A. W. Zand, and I. S. Abbood. "Peak ground acceleration models predictions utilizing two metaheuristic optimization techniques". Latin American Journal of Solids and Structures, 19.3, 1–23. 2022. https://doi.org/10.1590/1679-78256940
[10] Contents, T. O. F. 2014. "journal of physics and chemistry of". 1.1, 1–11.
[11] X. Liu, L. Jiang, P. Xiang,, and Z. Lai 2023. "safety and comfort assessment of a train passing over an earthquake-damaged bridge based on a probability model". Structure and Infrastructure Engineering, 19.4, 525–536. https://doi.org/10.1080/15732479.2021.1956549

[12] W. Khaerunnisa, N. S. J., Sujarmanto, I. S., and B. Michelle "Shifting perceptions of the locals after reclamation": The Ternate Historic Coastal City, Indonesia. ISVS E-Journal, 9.4, 145–160. 2022

[13] S. M. Y. Arafat, S. K.. Kar, and R. Kabir. 2022. "Panic buying and environmental disasters: management and mitigation approaches. panic buying and environmental disasters": Management and Mitigation Approaches, Sept., 1–320. https://doi.org/10.1007/978-3-031-10278-3

[14] A.P., Nugroho, B. Tohari. 2022. "A hybrid k-means hierarchical algorithm for natural disaster mitigation clustering". Journal of Information

[15] N. S. Kwong, K. S. Jaiswal, J. W. Baker, N. Luco, K. A. Ludwig, and V. J. Stephens. "Earthquake risk of gas pipelines in the conterminous united states and its sources of uncertainty". ASCE-ASME Journal of Risk and Uncertainty in Engineering Systems, Part A: Civil Engineering, 8.1, 1–22. 2022. https://doi.org/10.1061/ajrua6.0001202

[16] A. R Wijaya. "The spatio-temporal etas model in the analysis of earthquake intensity mapping in the sumatra region". Jambura Journal of Mathematics, 5.1, 179–188. 2023. https://doi.org/10.34312/jjom.v5i1.17359

[17] K.. Risk, O. On, and P. System 2022. "Assessment of operational risk on the development". 1–10.

[18] A. F. Putra, P. Chenrai . 2022. "Relative tectonic activity assessment of the northern sumatran fault using geomorphic indices". Frontiers in Earth Science, 10 August, 1–22. https://doi.org/10.3389/feart.2022.969170

[19] B.A. Ruzinov, 2022. "Akshikent earthquake". 9, 209–212.

[20] M. A. Soltane, M. Mimoune, and A. Guettiche .2022. "Earthquake-induced impact scenario assessment for the historical center of Skikda, Algeria". In Bulletin of Earthquake Engineering . Vol. 20, Issue 11. Springer Netherlands. https://doi.org/10.1007/s10518-022-01437-5

[21] D. Syafriani, S. Fikri, and Q. Guvil. 2022. "Monitoring of land surface change in Padang city using dinsar sentinel-1a method". *Journal of Applied Geospatial Information*, *6*.2, 615–619. 2022. https://doi.org/10.30871/jagi.v6i2.4134